A Tunable subTHz Source Based on the Josephson Oscillator with Phase Locking

Nickolay V. Kinev
Laboratory of Superconducting Devices for Signal Detection and Processing
Kotel'nikov Institute of Radio Engineering and Electronics of RAS
Moscow, Russia
nickolay@hitech.cplire.ru

Kirill I. Rudakov
Kapteyn Astronomical Institute
University of Groningen
Groningen, the Netherlands
rudakov@astro.rug.nl

Lyudmila V. Filippenko
Laboratory of Superconducting Devices for Signal Detection and Processing
Kotel'nikov Institute of Radio Engineering and Electronics of RAS
Moscow, Russia
lyudmila@hitech.cplire.ru

Valery P. Koshelets
Laboratory of Superconducting Devices for Signal Detection and Processing
Kotel'nikov Institute of Radio Engineering and Electronics of RAS
Moscow, Russia
valery@hitech.cplire.ru

***Abstract*—We present a new implementation for a sub-terahertz and terahertz source based on a superconducting Josephson flux-flow oscillator. The oscillator has been integrated with the transmitting antenna on a single chip providing the emission to open space, and with a harmonic mixer based on a superconductor-insulator-superconductor junction for a frequency and phase locking. We have used the double slot antenna to couple the oscillator output planar transmission line with the open space; the antenna is additionally matched to the elliptical silicon lens forming narrow output beam of subTHz radiation. The design of antenna and matching structures coupled to the oscillator has been developed and fabricated, the operating range 0.25 - 0.45 THz has been obtained experimentally.**

Keywords—terahertz radiation, superconducting integrated circuits, Josephson junctions, transmitting antennas, harmonic mixers

I. Introduction

The lack of easy tunable wideband terahertz (THz) and sub-terahertz (subTHz) sources nowadays is an important problem in astronomy, spectroscopy, radio science and other fields. The superconducting flux-flow oscillator (FFO) based on a long Josephson tunnel junction made of trilayers $Nb/AlO_x/Nb$ or Nb/AlN/NbN was successfully implemented as the local on-chip oscillator in the superconducting integrated receiver (SIR) [1-2] and proved to be a perspective solution for an easily tuned and ultra wideband source. It has an operating bandwidth of about 100% of central frequency: from 250 GHz to 700 GHz for the sample having the length of 400 μm and the width of 16 μm; the free-running spectral linewidth is about several MHz with Lorentzian shape [3-4]. The upper operating frequency can potentially reach 1.2 THz if NbTiN-based output transmission lines are used. Typically the phase locking loop (PLL) is used for such oscillator, for this purpose a small part of the output power is branched to the harmonic mixer (HM) based on a superconductor-insulator-superconductor (SIS) Josephson junction. The phase locking leads to an actual linewidth less than 100 kHz, which satisfy almost all needs for THz applications. The typical power of FFO is about 0.1 – 1 μW and can be increased by using larger current density of the Josephson junction. Recently we developed and elaborated the concept of integration of the FFO with the transmitting antenna and the HM for the frequency band 0.4 – 0.7 THz [5-7], this range is nearly covered by operating range of the SIR, thus the output emission of experimental samples of the developed designs were successfully studied by the SIR. In this paper, we have developed the antenna design having operating frequencies lower than 0.45 THz which is out the SIR operating range, therefore another technique for study of the emission to open space is required.

The study is supported by the Russian Science Foundation (project No. 17-79-20343).

II. Layout of the Oscillator and Numerical Simulations

A. Concept & Layout

The output frequency f of the FFO is strictly defined by the Josephson equation

$$hf = 2eV_{DC}\,, \tag{1}$$

where V_{DC} is the DC voltage on the junction. The operation of such oscillator is discussed elsewhere [7,8]; the bias current and the control line current for supplying the local magnetic field are used for setting V_{DC} and hence the operation frequency f. The layout of the proposed oscillator based on the FFO is shown in Fig. 1. The main idea of this study is the integration of the FFO with the HM for the feedback locking loop and with a transmitting slot antenna on a single microchip (Fig. 1a) placed on the back surface of the elliptical lens (Fig. 1b). The chip substrate and the lens are both made of silicon. Both tunnel junctions the FFO and the HM are to be fabricated of $Nb/AlO_x/Nb$ or Nb/AlN/NbN, top and bottom electrodes constitute the microstrip transmission lines. A similar type of double slot lens antenna was successfully used in [7] for higher frequencies, and the same semielliptical lens was used in [1,2,7] forming the narrow output beam having a width of the central lobe of a few degrees.

978-1-7281-0689-2/19/$31.00 ©2019 IEEE

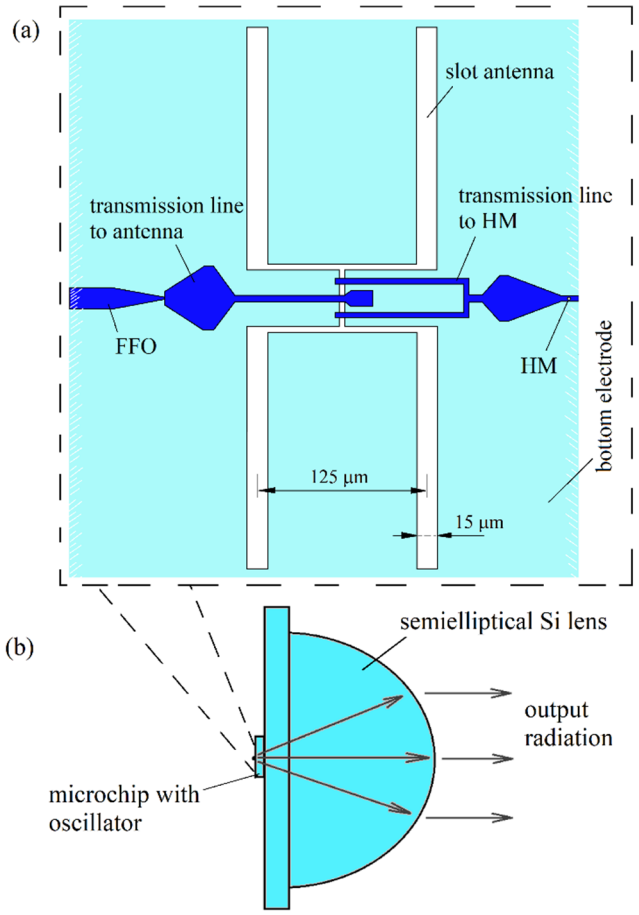

Fig. 1. (a) Layout of the planar microcircuit containing the FFO, double slot antenna, harmonic mixer and the coupling structures between the elements. (b) Scheme of the microchip with oscillator and antenna shown on (a) placed at the far focus of the silicon lens.

B. *Impedance of the Antenna*

The numerical simulations were carried out using the three-dimensional microwave modeling software. The emitting edge of the FFO was simulated as the input port #1 with the constant impedance of 0.5 Ω, and the HM was simulated as a port #2 with the impedance equaled to the normal resistance of the junction. This resistance is about 25 Ω and defined by the current density of a real trilayer (typically 5 – 10 kA/cm^2) and the area of the junction, which is expected to be 1.4 μm^2. The capacity of the HM was taken into account by embedding a capacitor in parallel to the port #2 according to specific capacitance 85 fF/μm^2. The mictrostrip line behind the HM contains the rf-short (not shown in Fig. 1a) in the form of radial stub to prevent the leakage of THz power beyond the HM. Then the microstrip line transforms to a CPW line for proper connection to the contact pads of the chip.

As the simulation task, we chose the central frequency of antenna operation to be about 300 GHz. A bandwidth of slot antenna is usually not more than ~0.5 of the central frequency. The calculated impedance of developed antenna design is presented in Fig. 2.

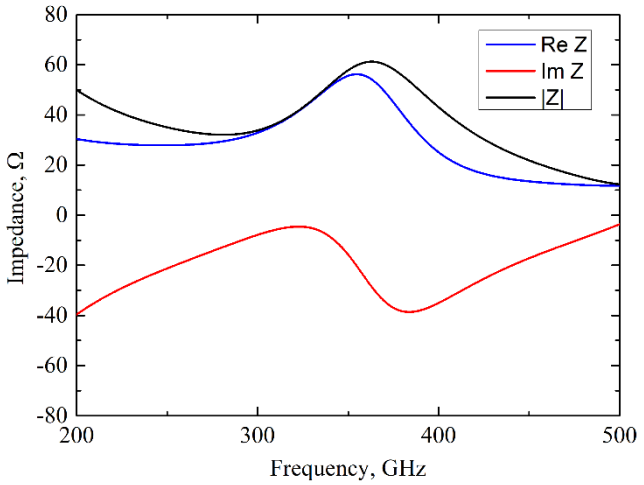

Fig. 2. Impedance Z of the antenna in the point of feeder connection: the real part Re Z, the imaginary part Im Z and the full impedance |Z| are shown.

C. *Power matching*

The numerical task is the coupling of the oscillator having low output impedance (less than 1 Ω) to the lens antenna having high impedance (tens of Ω) and forming a beam pattern required for applications, and simultaneous coupling to the HM having some intermediate impedance. Coupling to the antenna should be as high as possible, while coupling to the HM should be just enough for properly PLL operation (commonly 10-20% of total output power of the FFO) and should not take away much power. Both couplings with the antenna and the HM should be in the same frequency range, which is desired to be as wide as possible. The numerical results for the emission to open space and the coupling with the HM are illustrated in Fig. 3. According to these results, the operating range defined as the range with emission level to the open space higher than 0.7 of total FFO power is 250 – 420 GHz; this bandwidth (170 GHz) exactly corresponds to 0.5 of the central frequency 330 GHz. The power absorbed by the HM of about 0.05 - 0.12 is expected to be enough for locking the oscillator [3,4].

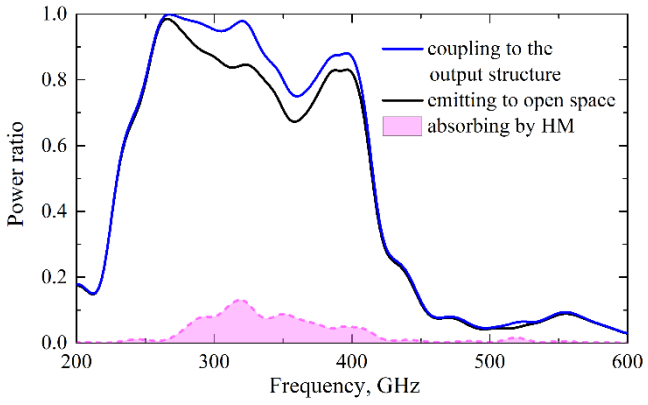

Fig. 3. The coupling of the FFO to the output structure (solid blue curve), emission power to open space (solid black curve) and the absorption by the HM (dashed magenta curve) for the developed integrated structure shown in Fig. 1a. The power is normalized to the total output FFO power. The area under the dashed curve is filled for clarity.

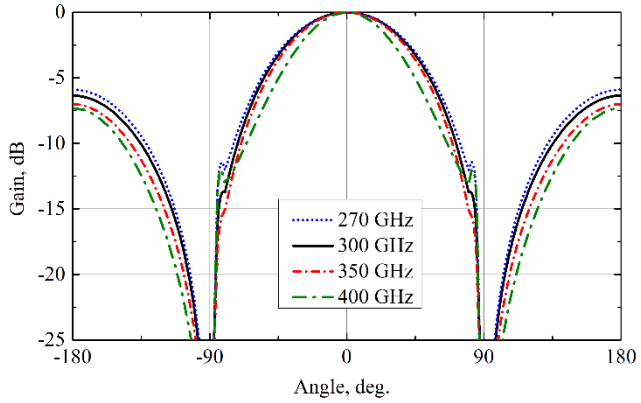

Fig. 4. Calculated beam patterns of the antenna at some frequencies in operating range.

D. Beam diagrams

In the Fig. 4 the calculated beam patterns for the integrated structure with antenna are shown for the set of frequencies in operating range, the main power is concentrated in the center lobe. The diagram has almost no change with change of frequency. Beam pattern calculations are made taking into account the silicon chip substrate and not taking into account the elliptical lens which greatly narrows and gains the central lobe [1], and has no influence on the dependence in Fig. 3.

III. Experiment

A. Samples Preparation

The technology for fabrication of samples containing integrated circuits with Nb/AlO_x/Nb tunnel junctions, with ~μm and sub-μm dimensions, has been described, e.g., in [9]. The key technology processes are an electron-beam lithography for mask preparation, a magnetron sputtering and a "lift-off" lithography. In this study, 4×4-mm^2 chips with developed circuits containing the subTHz antenna, the FFO and the HM based on Nb/AlO_x/Nb trilayers, were fabricated on a silicon substrate. The current density of the SIS trilayes on the batch is about $j_c = 8$ kA/cm^2, this corresponds to parameter R_nS of about 25 Ω·μm^2; the gap voltage V_g is about 2.7 mV, and the quality factor of the HM junctions defined as the ratio of "sub-gap" resistance to normal resistance R_j/R_n is about 30 for the best samples.

B. Results and Discussion

The DC measurements for superconducting structures are carried out by the dipstick testing in the liquid helium. The six contact pads are used for fully controlling the FFO with a four-point biasing current-control scheme ($+I_{BIAS}$, $+V_{BIAS}$, $-I_{BIAS}$, $-V_{BIAS}$) and an additional two-point control line scheme for applying the magnetic field ($+I_{CL}$, $-I_{CL}$). The HM is controlled via a four-point biasing voltage-control scheme.

A set of the current-voltage curves (IVCs) of fabricated FFOs measured for different magnetic fields produced by I_{CL} in the range 20 - 90 mA with a step size of 1 mA (71 curves altogether), is presented in Fig. 5. The axis of voltage strictly corresponds to the frequency of oscillator by factor 483.6 GHz/mV according to (1). The color of the curves indicate the pumping level of the HM, where blue color means no or weak pumping, and red color means strong pumping. The describing of the pumping current is given in the next paragraph.

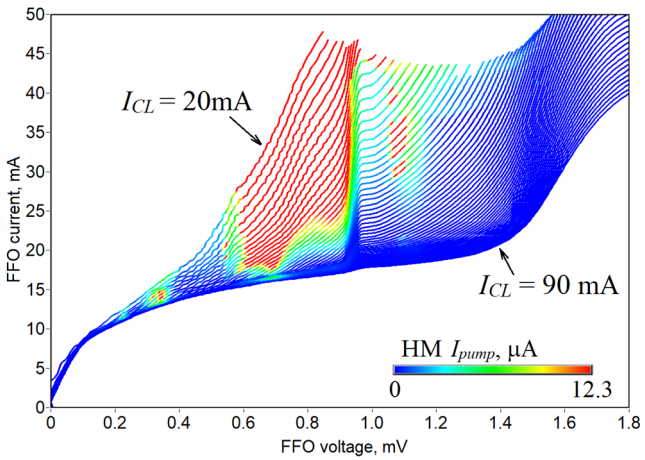

Fig. 5. IVCs of the FFO with the dimensions 700×16 μm^2 measured for different magnetic fields produced by the control line current with an I_{CL} step of 1 mA.

The pumping of the HM by the FFO power leads to the appearance of the quasiparticle step I_{pump} on the IVC of the HM that is shown in Fig. 6 on the set of IVCs w/o and with pumping. Thus, the pumping efficiency of the HM by the FFO has been measured as the quasiparticle step at some fixed sub-gap voltage on the IVCs of the HM in the whole operating range of the FFO, usually the HM operating point 2.5 mV is used for Nb/AlO_x/Nb junctions. The results for the HM pumping in comparison with the calculation results are presented in Fig. 7. The step is normalized to the "current jump" I_{gap} at V_g voltage, which is about 100-150 μA and is measured accurately for the specific junction. One can note a good agreement of the experiment with the numerical simulations.

In paper [7] we have successfully investigated the emission to open space of the FFO integrated with transmitting slot lens antenna designed for operating ranges with 450 GHz and 600 GHz central frequencies utilizing the THz spectrometer based on the SIR. For the design developed in this paper, the existing SIR is not appropriate instrument to measure the output emission since its operating range is above 450 GHz. Therefore we are planning to carry out the experiment for detecting of the emission to open space using

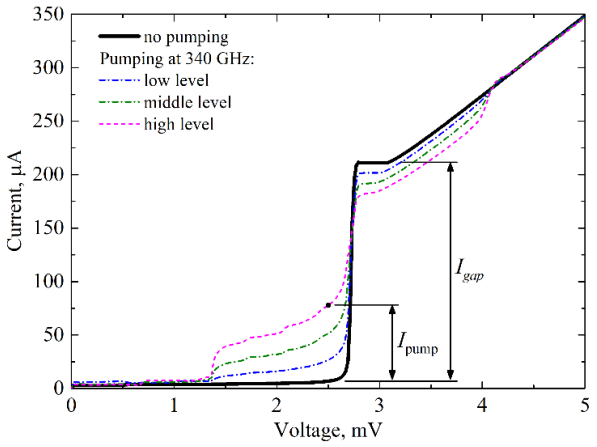

Fig. 6. IVCs of HM without external emission (solid curve) and with pumping by FFO power at fixed frequency 340 GHz and different pumping power (dashed curves). A "current jump" I_{gap} at V_g voltage, and a pumping current I_{pump} at V=2.5mV are shown for black and magenta curves respectively.

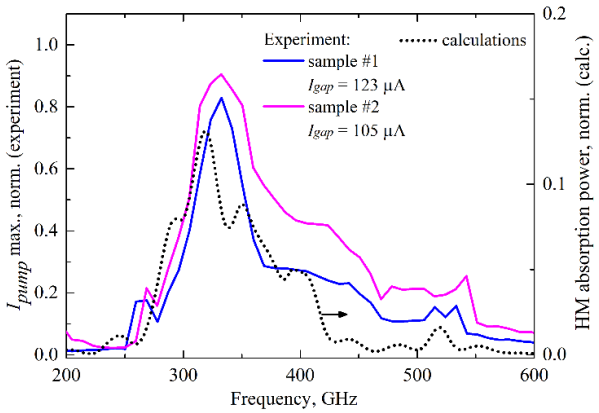

Fig. 7. HM pumping by FFO power (solid curves) measured experimentally for two samples and numerical results of the absorbed FFO power by HM (dot curve). The HM pumping current is normalized to I_{gap}; the absorbed power is normalized to the total output FFO power. The dot curve is the same as the dashed curve in Fig. 3.

the cooled Si bolometer as the direct detector; the infrared filers should be used to measure subTHz and THz signal. This technique is good to measure the emitting power in the whole frequency operation range to compare with numerical results in Fig. 3, however the Si bolometer does not allow to resolve the spectra. At the same time, spectral characteristics of the FFO are defined by the slope of IVCs (spectral linewidth is proportional to squared differential resistance of the junction R_d^2 at the point of operation), and were already studied in [3,4,7]. So, the spectral linewidth of the oscillator of experimental samples developed in this paper in the range of 250-420 GHz at a Fiske step regime is expected to be 1 - 5 MHz with a Lorentzian shape in free-running regime for Nb/AlO_x/Nb structures.

IV. Conclusions

The superconducting THz and subTHz oscillator based on a unidirectional flow of the fluxons in a long Josephson junction (a flux-flow oscillator or a FFO) is a promising solution of the THz/subTHz source for the tasks where wideband frequency tuning is required and the high power is not necessary. We have presented the implementation for the external subTHz source based on the FFO integrated with the harmonic mixer and the transmitting slot antenna on a single chip. The lens is used forming the narrow beam pattern. The design of the antenna, HM and transmission lines for 0.25 - 0.42 THz region is numerically simulated and studied experimentally. The experimental samples based on Nb/AlO_x/Nb trilayers with current density of about 8 kA/cm^2 and gap voltage of 2.7 mV have been fabricated. The pumping of the HM is measured for a several samples in the whole region of FFO operation. The calculations are in a good agreement with the experiment.

References

[1] G. de Lange et al., "Development and characterization of the superconducting integrated receiver channel of the TELIS atmospheric sounder," Supercond. Sci. Technol., vol. 23, No. 4, pp. 045016-1 – 045016-8, March 2010.

[2] V. P. Koshelets et al., "Superconducting Integrated Terahertz Spectrometers," IEEE Trans. Terahertz Sci. Technol., vol. 5, Iss. 4, pp. 687–694, July 2015.

[3] V. P. Koshelets et al., "Line width of Josephson flux flow oscillators," Physica C, vol. 372–376, No. 1, pp. 316–321, August 2002.

[4] V. P. Koshelets et al., "Towards a phase-locked superconducting integrated receiver: prospects and limitations," Physica C, vol. 367, Iss. 1–4, pp. 249–255, February 2002.

[5] N. V. Kinev, K. I. Rudakov, A. M. Baryshev, and V. P. Koshelets, "Slot lens antenna based on thin nb films for the wideband josephson terahertz oscillator," Phys. Solid State, vol. 60, Iss. 11, pp. 2173–2177, November 2018.

[6] N. V. Kinev, K. I. Rudakov, L. V. Filippenko, A. M. Baryshev, and V. P. Koshelets, "Wideband Josephson THz flux-flow oscillator integrated with the slot lens antenna and the harmonic mixer," EPJ Web Conf., vol. 195, pp. 02003-1–02003-2, November 2018.

[7] N. V. Kinev , K. I. Rudakov, L. V. Filippenko, A. M. Baryshev, and V. P. Koshelets, "Flux-flow Josephson oscillator as the broadband tunable terahertz source to open space," J. Appl. Phys., vol. 125, pp. 151603-1–151603-7, March 2019.

[8] T. Nagatsuma, K. Enpuku, F. Irie, and K. Yoshida, "Flux-flow type Josephson oscillator for millimeter and submillimeter wave region," J. Appl. Phys., vol. 54, pp. 3302–3309, February 1983.

[9] L. V. Filippenko et al., "Submillimeter superconducting integrated receivers: fabrication and yield," IEEE Trans. on Appl. Supercond., vol. 11, Iss. 1, pp. 816–819, March 2001.